chemengineering

MDPI

Article

Successive Crystallization of Organically Templated Uranyl Sulfates: Synthesis and Crystal Structures of $[pyH](H_3O)[(UO_2)_3(SO_4)_4(H_2O)_2]$, $[pyH]_2[(UO_2)_6(SO_4)_7(H_2O)]$, and $[pyH]_2[(UO_2)_2(SO_4)_3]$

Evgeny V. Nazarchuk [1,*], Dmitri O. Charkin [2] and Oleg I. Siidra [1,3]

[1] Department of Crystallography, Saint-Petersburg State University, University emb. 7/9, St. Petersburg 199034, Russia; o.siidra@spbu.ru
[2] Department of Chemistry, Moscow State University, GSP-1, Moscow 119991, Russia; d.o.charkin@gmail.com
[3] Kola Science Center, Russian Academy of Sciences, Apatity 184200, Russia
* Correspondence: e_nazarchuk@mail.ru; Tel.: +7-911-156-14-79

Abstract: Three new uranyl sulfates, $[pyH](H_3O)[(UO_2)_3(SO_4)_4(H_2O)_2]$ (**1**), $[pyH]_2[(UO_2)_6(SO_4)_7(H_2O)]$ (**2**), and $[pyH]_2[(UO_2)_2(SO_4)_3]$ (**3**), were produced upon hydrothermal treatment and successive isothermal evaporation. **1** is monoclinic, $P2_1/c$, a = 14.3640(13), b = 10.0910(9), c = 18.8690(17) Å, β = 107.795(2), V = 2604.2(4) Å^3, R_1 = 0.038; **2** is orthorhombic, $C222_1$, a = 10.1992(8), b = 18.5215(14), c = 22.7187(17) Å, V = 4291.7(6) Å^3, R_1 = 0.030; **3** is orthorhombic, $Pccn$, a = 9.7998(8), b = 10.0768(8), c = 20.947(2) Å, V = 2068.5(3) Å^3, R_1 = 0.055. In the structures of **1** and **2**, the uranium polyhedra and SO_4 tetrahedra share vertices to form $^3_\infty[(UO_2)_3(SO_4)_4(H_2O)_2]^{2-}$ and $^3_\infty[(UO_2)_6(SO_4)_7(H_2O)]^{2-}$ frameworks featuring channels (12.2 × 6.7 Å in **1** and 12.9 × 6.5 Å in **2**), which are occupied by pyridinium cations. The structure of **3** is comprised of $^2_\infty[(UO_2)_2(SO_4)_3]^{2-}$ layers linked by hydrogen bonds donated by pyridinium cations. The compounds **1**–**3** are formed during recrystallization processes, in which the evaporation of mother liquor leads to a stepwise loss of hydration water.

Keywords: uranyl sulfates; organically templated compounds; pyridinium; framework structures; crystal engineering

Citation: Nazarchuk, E.V.; Charkin, D.O.; Siidra, O.I. Successive Crystallization of Organically Templated Uranyl Sulfates: Synthesis and Crystal Structures of $[pyH](H_3O)[(UO_2)_3(SO_4)_4(H_2O)_2]$, $[pyH]_2[(UO_2)_6(SO_4)_7(H_2O)]$, and $[pyH]_2[(UO_2)_2(SO_4)_3]$. *ChemEngineering* **2021**, *5*, 5. https://doi.org/10.3390/chemengineering5010005

Received: 17 November 2020
Accepted: 10 January 2021
Published: 20 January 2021

1. Introduction

Microporous uranium compounds formed upon the oxidation of spent nuclear fuel (SNF) attract essential interest due to their non-trivial crystal chemistry [1], and they also are promising materials for ion exchange and catalysis [2–6]. For instance, framework uranyl phosphates selectively absorb ^{90}Sr and ^{137}Cs nuclides [7–9]. The largest structural diversity is observed among compounds containing tetrahedral and pseudo-tetrahedral oxo-anions, e.g., molybdates [10–16], phosphonates [17], phosphates [18–21], and vanadates [22,23]. Examples of non-trivial structures also exist among uranyl sulfates [24–27] and chromates [28]. The increasing interest in uranyl sulfates stems mostly from their prominent role in the oxidation of uranium deposits and the formation of various secondary minerals [29,30], as well as from their potential use in SNF processing [31]. Several approaches to the preparation of open-framework uranyl compounds have been developed [13–28] whereof hydrothermal synthesis is the most common [32].

A variety of positively charged species, both organic and inorganic, have been employed in templating the uranyl-based inorganic frameworks, as the latter are generally negatively charged. As yet, the relationships between the nature of the cationic species and structure and composition of inorganic counterparts and total outcome are rather vague, so new structures are expected to help further understanding and subsequent targeted synthesis. Their composition and structures are likely to depend not only on the initial ratio of the reactants but also on their absolute and relative concentrations

which are expected to vary also in the case of sequential crystallization. These phenomena have been monitored in a relatively small number of systems studied. Hereby, we report on the synthesis and crystal structures of three new uranyl sulfates templated by pyridinium cations, $[pyH](H_3O)[(UO_2)_3(SO_4)_4(H_2O)_2]$ (**1**), $[pyH]_2[(UO_2)_6(SO_4)_7(H_2O)]$ (**2**), and $[pyH]_2[(UO_2)_2(SO_4)_3]$ (**3**), which were successively produced by hydrothermal treatment with subsequent isothermal evaporation. We discuss the peculiarities of their crystal structures as well as the templating effect of pyridinium cations.

2. Synthesis

Caution! While the compounds of depleted uranium are only weakly radioactive, their chemical toxicity is essential. All safety regulations should be followed strictly.

Crystals of **1–3** were grown from a solution containing 0.5 g of $(UO_2)(NO_3)_2{\cdot}6H_2O$ (Vekton, 99.7%), 2 mL of H_2SO_4 (Vekton, 99.7%), 0.01 mL of pyridine (Aldrich, 99.5%), and 5ml of H_2O. It was heated at 220 °C in a Teflon-lined autoclave under autogeneous pressure for two weeks. The transparent yellow solution was allowed to slowly evaporate in air in a fume hood. The crystals formed within 3–10 days. Those of **1** appear at pH ≈ 2.5 as spherical aggregates (Figure 1a,b). Further evaporation leads to the dissolution of surface crystals; at pH = 2 to 1.5, they transform into crystals of **2** (Figure 1c), so that both **1** and **2** coexist on the surface of the spherical aggregates until pH ≈1. The structural studies (vide infra) indicate that the conversion of **1** into **2** leads to the loss of one molecule of hydration water.

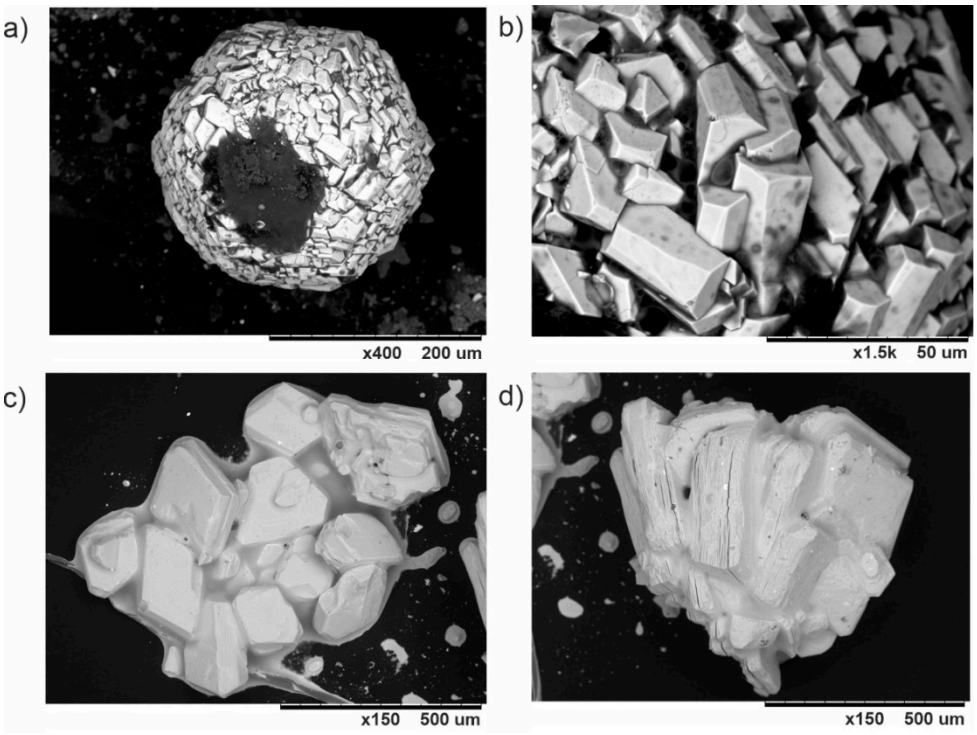

Figure 1. Micrographs of the crystals of **1** (**a**,**b**), **2** (**c**), and **3** (**d**).

At pH ≈ 1, the crystals of **1** and **2** completely dissolve, after which the platelets of **3** (Figure 1d) are formed within 12 h. Further evaporation leads to complete drying without any other transformations. Qualitative electron microprobe analysis of **1–3** (LINK AN-10000 EDS system) revealed no other elements, except U and S, with an atomic number greater than 11 (Na).

Single-Crystal Studies

Selected single crystals were attached to glass fibers using an epoxy resin and mounted on a Bruker SMART APEX II DUO diffractometer equipped with a micro-focus X-ray tube utilizing Mo*K* radiation. The experimental datasets were collected at 100K. Unit cell parameters were calculated using least-squares fits. Structure factors were derived using APEX 2 after introducing the required corrections. Crystal structures were solved using direct methods. The final model includes site coordinates and anisotropic thermal parameters for all atoms except hydrogens, which were localized using AFIX command in calculated positions (d(A-H) = 1.00(1) Å). Hydrogen atoms of the water molecules could not be localized. Further details are collected in Table 1. Crystals of **3** were found to be unstable under the X-ray beam and decompose within 1.5 h.

Table 1. Crystallographic data and refinement parameters for [pyH](H_3O)[(UO_2)$_3$(SO_4)$_4$(H_2O)$_2$] (**1**), [pyH]$_2$[(UO_2)$_6$(SO_4)$_7$(H_2O)] (**2**), and [pyH]$_2$[(UO_2)$_2$(SO_4)$_3$] (**3**). Experiments were carried out at 100 K with MoKα radiation on Bruker Smart DUO CCD.

Compound	**1**	**2**	**3**
Crystal system	Monoclinic	orthorhombic	orthorhombic
Space group	$P2_1/c$	$C222_1$	$Pccn$
Unit cell dimensions	14.3640(13) 10.0910(9)	10.1992(8) 18.5215(14)	9.7998(8) 10.0768(8)
a, b, c (Å)	18.8690(17)	22.7187(17)	20.947(2)
β (°)	107.795(2)	90	90
Unit-cell volume (Å^3)	2604.2(4)	4291.7(6)	2068.5(3)
Z	2	4	4
Calculated density (g·cm^{-3})	3.383	3.846	3.174
Absorption coefficient (mm^{-1})	19.037	23.026	16.027
Crystal size (mm)	0.10 × 0.15 × 0.13	0.14 × 0.09 × 0.13	0.14 × 0.20 × 0.11
Data collection			
Radiation, wavelength (Å)	Mo$K\alpha$, 0.71073	Mo$K\alpha$, 0.71073	Mo$K\alpha$, 0.71073
F(000)	2396	6500	1800
θ range (°)	2.27–28.00	2.20–33.05	2.81–35.84
h, k, l ranges	−18→12 −13→13 −24→24	−15→15 −28→27 −34→31	−12→2 −12→6 −9→24
Total reflections collected	24039	19596	2249
Unique reflections (R_{int})	6292(0.051)	7635(0.0383)	1728(0.0242)
Unique reflections $F > 4\sigma(F)$	5287	6519	1401
Structure refinement			
Refinement method	Full-matrix least-squares on F^2	Full-matrix least-squares on F^2	Full-matrix least-squares on F^2
Weighting coefficients a, b	0.0383, 20.0641	0.008, 0.00	0.1368, 3.3627
Data/restraints/parameters	6292/0/351	7635/0/304	1728/6/123
R_1 [$F > 4\sigma(F)$], wR_1 [$F > 4\sigma(F)$]	0.032, 0.077	0.030, 0.055	0.055, 0.167
R_2 all, wR_2 all	0.043, 0.086	0.043, 0.052	0.067, 0.190
Gof on F^2	1.037	0.966	1.084
CCDC	2036077	2036078	2036079

3. Results

The crystal structures of **1** and **2** contain three symmetrically independent uranium atoms, while only one is in the structure of **3** (Figure 2). In all cases, typical uranyl cations (*Ur*) are formed (<d(U–O)> = 1.751, 1.756, 1.773, 1.755, 1.745, 1.751 and 1.770 Å, respectively; see Figure 2). In **1**, *Ur*(1) coordinates five oxygen atoms from the sulfate anions in the equatorial plane, while *Ur*(2) and *Ur*(3) coordinate four sulfate oxygens and one water molecule.

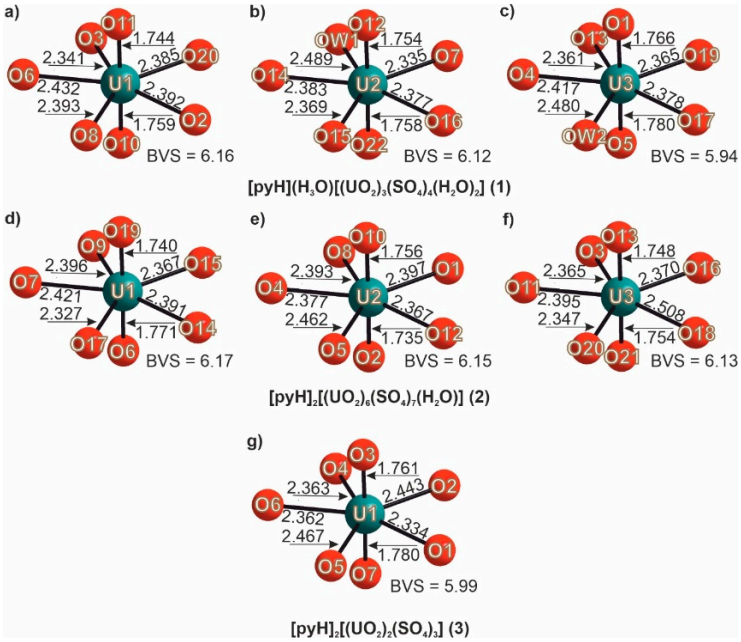

Figure 2. Coordination of uranium in **1**(**a**–**c**), **2**(**d**–**f**), and **3**(**g**).

The *Ur*-H_2O distances ($d(Ur(2)–H_2O)$ = 2.489 Å, $d(Ur(3)–H_2O)$ = 2.480 Å) are slightly longer compared to the *Ur*-O from the sulfate tetrahedra (<d(U–O)> = 2.379 Å). In the structures of **2** and **3**, the uranyl cations bond only to the sulfate oxygens forming the classical UrO_5 pentagonal bipyramids (<d(U–O)> = 2.392 and 2.395 Å in **2** and **3**, respectively). The structures of **1** and **2** also contain four independent sulfur atoms, while in **3**, ther are only two that center the sulfate tetrahedra (<d(S–O)> = 1.473, 1.465 and 1.473 Å, for **1**, **2**, and **3** respectively).

The bond valence sums (BVS) for U^{VI} and S^{VI} (Figures 2 and 3) were calculated using parameters given in [33] and [34], respectively. They are in proper agreement to the reference data [1].

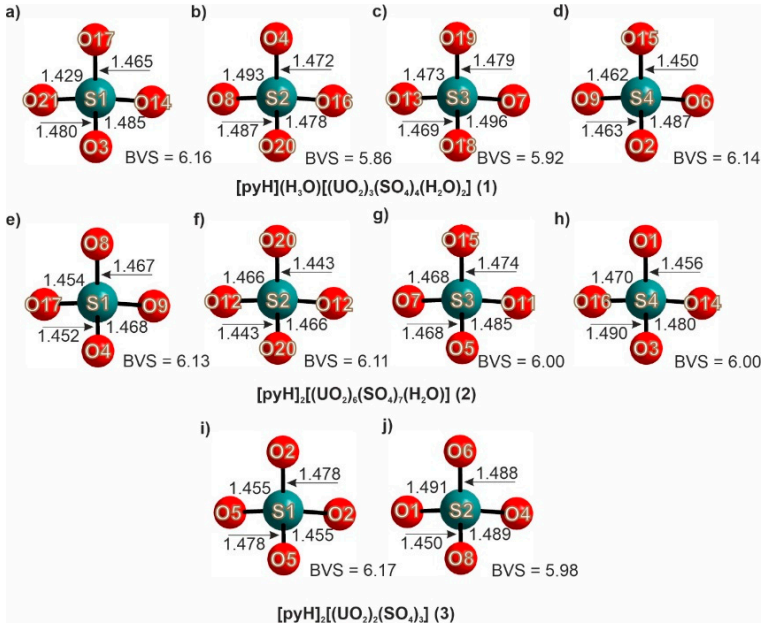

Figure 3. Coordination of sulfur in **1** (**a**–**d**), **2** (**e**–**h**), and **3** (**i**,**j**).

In **1**, the UO_7 and SO_4 moieties share corners to form a $^3_\infty[(UO_2)_3(SO_4)_4(H_2O)_2]^{2-}$ framework (Figure 4a) with 12.2 × 6.7 Å channels running along [100]. These channels are occupied by pyridinium and disordered hydronium cations as well as water molecules. Following the description of uranyl molybdate [10–16] and vanadate [23] frameworks, that of **1** can be described as being constructed of $^1_\infty[(UO_2)_2(SO_4)_3]^{2-}$ ribbons linked by $[(UO_2)_2(SO_4)_2(H_2O)_2]$ groups (Figure 4b). The $^1_\infty[(UO_2)_2(SO_4)_3]^{2-}$ ribbons (Figure 4c) are in their turn comprised of *C*1 and *C*1′ chains used in the description of nanotubules in the structure of $Na(C_8H_{10}NO_2)_7[(UO_2)_6(SO_4)_{10}]\cdot 3.5H_2O$ [35].

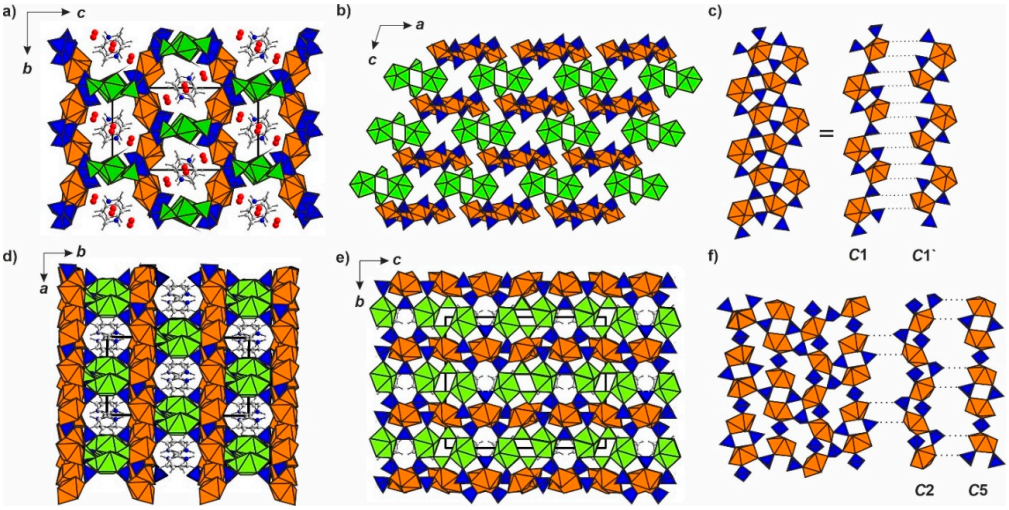

Figure 4. Projection of the structure of **1** onto *bc* (**a**) and *ac* (**b**); The $^1_\infty[(UO_2)_2(SO_4)_3]^{2-}$ ribbons (**c**), formed from *C*1 and *C*1′ chains. Projection of 2 onto *ab* (**d**) and *bc* (**e**); the $^2_\infty[(UO_2)_2(SO_4)_3]^{2-}$ layers (**f**) are comprised of *C*2 and *C*5 chains. The linking $[(UO_2)(SO_4)_2(H_2O)_2]$ groups are highlighted in green.

In **2**, the UO_7 and SO_4 polyhedra also share corners to form a $^3_\infty[(UO_2)_6(SO_4)_7(H_2O)]^{2-}$ framework with a more complex topology (Figure 4d). The UO_2:TO_4 = 6:7 frameworks had earlier been observed among uranyl sulfates [26] and molybdates [13,14,36]. The framework in **2** is comprised of $^2_\infty[(UO_2)_2(SO_4)_3]^{2-}$ layers pillared by $[(UO_2)(SO_4)_2]$ groups (Figure 4e). It contains 12.9 × 6.5 Å channels occupied solely by pyridinium species. Channels of such size are relatively common for the UO_2:SO_4 = 6:7 frameworks, e.g., 10.5 × 10.2 Å in $(n\text{-}C_4H_9NH_3)_2[(UO_2)_6(SO_4)_7(H_2O)_2]$ [25]. The topology of $^2_\infty[(UO_2)_2(SO_4)_3]^{2-}$ layers shown in Figure 4f is observed for the first time; yet, they can be "decomposed" into known *C*2 and *C*5 fundamental chains.

The structure of **3** (Figure 5a) contains $^2_\infty[(UO_2)_2(SO_4)_3]^{2-}$ layers with a relatively common topology known among uranyl selenates, [37], molybdates [38], chromates [39], and sulfates [37] (Figure 5b). The organic species occupy the interlayer gallery.

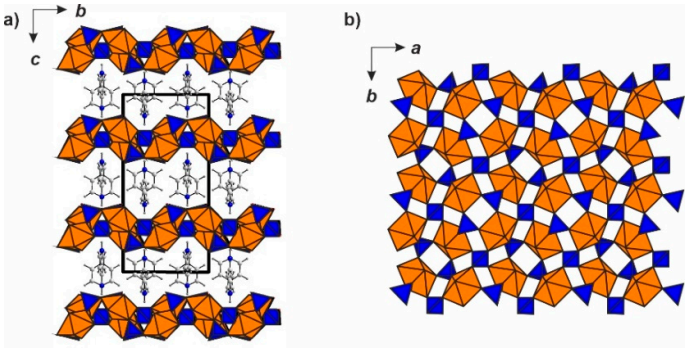

Figure 5. Projection of the structure of **3** onto *ab* (**a**) and $^2_\infty[(UO_2)_2(SO_4)_3]^{2-}$ layers in the 3 (**b**).

4. Discussion

In all three structures, the pyridinium cations form hydrogen bonds to the inorganic backbones (Figure 6). In **1** (Figure 6a), a bifurcated hydrogen bond is formed to the terminal (d(H1···O9) = 1.793 Å) and bridging (d(H1···O2) = 2.447 Å) oxygen atoms of the sulfate tetrahedra. In **2** (Figure 6b), these bonds are longer (d(H1···O6) = 2.523 Å, d(H1···O13) = 2.707 Å, and d(H1···O18) = 2.992 Å) and formed only to the equatorial atoms of the uranyl polyhedra (Figure 6b). In contrast, in **3,** two symmetrically independent pyridinium cations form different systems of hydrogen bonds (Figure 6c): one to the oxygens of the uranyl cations (d(H1···O3) = 2.146 Å), while the other is to the bridging oxygens of sulfate (d(H5···O5) = 2.144 Å).

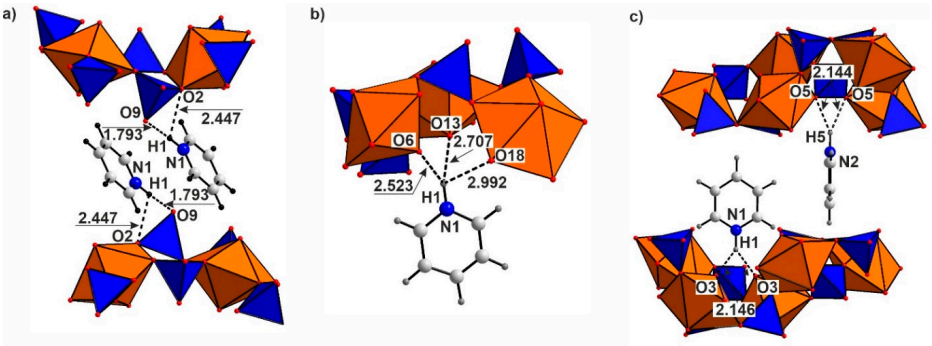

Figure 6. Hydrogen bonds in **1** (**a**), **2** (**b**), and **3** (**c**) shown as dashed lines.

A commonly addressed question is the effect of the organic species on the composition and topology of inorganic backbones where two opposite opinions have been expressed. On the one hand, the relatively small set of dominating inorganic structures suggests that the role of the positively charged organic matter is just to compensate the negative charge of the inorganic part [40]. On the other hand, the layers are sometimes strongly twisted or even rolled into nanotubes [24] due to the formation of organic micelles or other stable aggregates. In the structures of **1**–**3**, the pyridinium cations contribute to already known inorganic architectures; hence, their structure-driving role therein can be considered as modest. The least common is the 6:7 architecture wherein the size of the pyridinium cation most likely fits well the size of channels. This suggestion is tentative; to corroborate it, additional experiments seem to be desirable using the chemical analogs of pyridine. Yet, this structure is not produced when just slightly different 2- and 4-aminopyridimium cations are employed. Therefore, the shape requirements for this framework may be essential for rigid (e.g., aromatic) templates. The pyH^+ cations exhibit the common parallel or perpendicular stacking of aromatic rings, which is clearly seen in Figure 6a,c. The same stacking is suggested to be responsible for templating a much more complex nanotubular structure in $Na(C_8H_{10}NO_2)_7[(UO_2)_6(SO_4)_{10}]\cdot 3.5H_2O$ [35]. It is possible that electrostatic repulsion between the positively charged pyridinium cations may counteract the stacking. This repulsion between pyridinium rings is probably stronger in comparison to that between the anilinium parts of the phenylglycinium species in $Na(C_8H_{10}NO_2)_7[(UO_2)_6(SO_4)_{10}]\cdot 3.5H_2O$, which in neighbor cations point into different directions.

According to their chemical composition, compounds **1**–**3** formed upon successive crystallization contain decreasing amounts of crystallization water (two in **1**, one in **2,** and none in **3**). The authors of [28] calculated the densities of the frameworks comprised of uranyl cations and TO_4^{n-} tetrahedral oxyanions (FD) as the sum of U and T atoms per 1000 Å^3. The magnitudes vary from the minimum of FD = 8.54 for $(H_3O)_8(H_3O)$@(18-crown-6)$_2[(UO_2)_{14}(SO_4)_{19}(H_2O)_4](H_2O)_{20.5}$ [24] to the maximum of FD = 17.85 for $[(UO_2)(S_2O_7)]$ [41]. For the frameworks in $M[(UO_2)_3(MoO_4)_4(H_2O)_3](H_2O)_n$, (M = Mg, Zn, Ba; n = 3, 5) [36], the FD values are 10.89, 10.91, and 11.26, respectively. In the meantime, the FD value for the framework in **1** ($^3_\infty[([(UO_2)_3(SO_4)_4(H_2O)_2]^{2-}$) is 11.52. The increase of density as compared to the molybdate analog can be explained by lower hydration, as well

as by smaller size of the sulfate anion. The same is also true for the $^3_\infty[(UO_2)_6(TO_4)_7(H_2O)_2]$ frameworks. For the uranyl molybdate architectures [13–16], the FD values vary from 9.44 to 10.01, dependent on the nature of the cation. In the meantime, these values reach 11.94 and 12.11 for the frameworks in $(C_4H_{12}N)_2[(UO_2)_6(H_2O)_2(SO_4)_7]$ [26] and $(n\text{-}C_4H_9NH_3)_2[(UO_2)_6(SO_4)_7(H_2O)_2]$ [25]. For **2,** the FD is 12.12. For comparison, the calculated value for faujasite is 13.5. For the layered structure of **3**, FD = 9.67, which is close to the range observed for $^3_\infty[(UO_2)_6(MoO_4)_7(H_2O)_2]$ frameworks. Hence, successive recrystallization of the compounds under discussion leads first to the increase of the uranyl–sulfate framework (11.52→12.12) but to an essential drop on the second step (12.12→9.67), which correlates with the reduction of dimensionality.

Author Contributions: E.V.N. and O.I.S. designed the study, performed, and interpreted single crystal X-ray diffraction experiments; D.O.C. performed synthesis; E.V.N., O.I.S. and D.O.C. wrote the paper. All authors have read and agreed to the published version of the manuscript.

Funding: This work was financially supported by the Russian Science Foundation through the grant 16-17-10085.

Institutional Review Board Statement: Not applicable.

Informed Consent Statement: Not applicable.

Data Availability Statement: Data is contained within the article.

Acknowledgments: Technical support by the SPbSU X-ray Diffraction and Microscopy and Microanalysis Resource.

Conflicts of Interest: The authors declare no conflict of interest.

References

1. Krivovichev, S.V.; Burns, P.C.; Tananaev, I.G. *Structural Chemistry of Inorganic Actinide Compounds*; Elsevier: Amsterdam, The Netherlands, 2007; ISBN 9780444521118.
2. Albrecht-Schmitt, T.E. Actinide materials adopt curvature: Nanotubules and nanospheres. *Angew. Chem.* **2005**, *44*, 4836–4838. [CrossRef] [PubMed]
3. Shvareva, T.Y.; Skanthakumar, S.; Soderholm, L.; Clearfield, A.; Albrecht-Schmitt, T.E. Cs^+-selective ion exchange and magnetic ordering in a three-dimensional framework uranyl vanadium phosphate. *Chem. Mater.* **2007**, *19*, 132–134. [CrossRef]
4. Shvareva, T.Y.; Sullens, T.A.; Shehee, T.C.; Albrecht-Schmitt, T.E. Syntheses, structures, and ion-exchange properties of the three-dimensional framework uranyl gallium phosphates, $Cs_4[(UO_2)_2(GaOH)_2(PO_4)_4]\cdot H_2O$ and $Cs[UO_2Ga(PO_4)_2]$. *Inorg. Chem.* **2005**, *44*, 300–305. [CrossRef] [PubMed]
5. Halasyamani, P.S.; Francis, R.J.; Bee, J.S.; O'Hare, D. Variable dimensionality in the uranium fluoride/2-methyl-piperazine system: Syntheses and structures of UFO-5, 6, and 7; zero, one, and two dimensional materials with unprecedented topologies. In Proceedings of the Materials Research Society Symposium, San Francisco, CA, USA, 5–9 April 1999; Volume 547, pp. 383–388.
6. Doran, M.; Walker, S.M.; O'Hare, D. Synthesis and characterization of $(C_4N_2H_{12})(UO_2)_2(PO_3H)_2\{PO_2(OH)H\}_2$: A three dimensionally connected actinide framework. *Chem. Commun.* **2001**, *19*, 1988–1989. [CrossRef] [PubMed]
7. Kim, J.-Y.; Norquist, A.J.; O'Hare, D. $[(Th_2F_5)(NC_7H_5O_4)_2(H_2O)][NO_3]$: An actinide—Organic open framework. *J. Am. Chem. Soc.* **2003**, *125*, 12688–12689. [CrossRef] [PubMed]
8. Romanchuk, A.Y.; Vlasova, I.E.; Kalmykov, S.N. Speciation of uranium and plutonium from nuclear legacy sites to the environment: A mini review. *Front. Chem.* **2020**, *8*, 1–10. [CrossRef] [PubMed]
9. Ok, K.M.; Doran, M.B.; O'Hare, D. $[(CH_3)_2NH(CH_2)_2NH(CH_3)_2][(UO_2)_2F_2(HPO_4)_2]$: A new organically templated layered uranium phosphate fluoride-synthesis, structure, characterization, and ion-exchange reactions. *Dalton Trans.* **2007**, *30*, 3325–3329. [CrossRef]
10. Nazarchuk, E.V.; Siidra, O.I.; Krivovichev, S.V. Synthesis and crystal structure of $Ag_2[(UO_2)_6(MoO_4)_7(H_2O)_2](H_2O)_2$. *Radiochemistry* **2016**, *58*, 1–5. [CrossRef]
11. Nazarchuk, E.V.; Siidra, O.I.; Krivovichev, S.V.; Malcherek, T.; Depmeier, W. First mixed alkaline uranyl molybdates: Synthesis and crystal structures of $CsNa_3[(UO_2)_4O_4(Mo_2O_8)]$ and $Cs_2Na_8[(UO_2)_8O_8(Mo_5O_{20})]$. *Anorg. Allg. Chem.* **2009**, *635*, 1231–1235. [CrossRef]
12. Nazarchuk, E.V.; Krivovichev, S.V.; Burns, P.C. Crystal structure of $Tl_2[(UO_2)_2(MoO_4)_3]$ and crystal chemistry of the compounds $M_2[(UO_2)_2(MoO_4)_3]$ (M = Tl, Rb, Cs). *Radiochemistry* **2005**, *47*, 447–451. [CrossRef]
13. Krivovichev, S.V.; Burns, P.C.; Armbruster, T.; Nazarchuk, E.V.; Depmeier, W. Chiral open-framework uranyl molybdates. 1. Topological diversity: Synthesis and crystal structure of $[(C_2H_5)_2NH_2]_2[(UO_2)_4(MoO_4)_5(H_2O)](H_2O)$. *Microporous Mesoporous Mater.* **2005**, *78*, 217–224. [CrossRef]

14. Krivovichev, S.V.; Cahill, C.L.; Nazarchuk, E.V.; Armbruster, T.; Depmeier, W. Chiral open-framework uranyl molybdates. 2. Flexibility of the U:Mo = 6:7 frameworks: Syntheses and crystal structures of $(UO_2)_{0.82}[C_8H_{20}N]_{0.36}[(UO_2)_6(MoO_4)_7(H_2O)_2](H_2O)_n$ and $[C_6H_{14}N_2][(UO_2)_6(MoO_4)_7(H_2O)_2](H_2O)_m$. *Microporous Mesoporous Mater.* **2005**, *78*, 209–215. [CrossRef]
15. Krivovichev, S.V.; Armbruster, T.; Chernyshov, D.Y.; Burns, P.C.; Nazarchuk, E.V.; Depmeier, W. Chiral open-framework uranyl-molybdates. 3. Synthesis, structure and the $C222_1 \rightarrow P2_12_12_1$ low temperature phase transition of $[C_6H_{16}N]_2[(UO_2)_6(MoO_4)_7(H_2O)_2](H_2O)_2$. *Microporous Mesoporous Mater.* **2005**, *78*, 225–234. [CrossRef]
16. Nazarchuk, E.V.; Krivovichev, S.V.; Burns, P.C. Crystal structure and phase transformations of $Ca[(UO_2)_6(MoO_4)_7(H_2O)_2](H_2O)_n$ (n ~ 7.6). *Zap. Ross. Mineral.* **2005**, *134*, 110–117.
17. Yang, W.; Parker, T.G.; Sun, Z. Structural chemistry of uranium phosphonates. *Coord. Chem. Rev.* **2015**, *303*, 86–109. [CrossRef]
18. Doran, M.B.; Stuart, C.L.; Norquist, A.J.; O'Hare, D. $(C_8H_{26}N_4)_{0.5}[(UO_2)_2(SO_4)_3(H_2O)]_2H_2O$, an organically templated uranyl sulfate with a novel layer type. *Chem. Mater.* **2004**, *16*, 565–566. [CrossRef]
19. Danis, J.A.; Runde, W.H.; Scott, B.; Fettinger, J.; Eichhorn, B. Hydrothermal synthesis of the first organically templated open-framework uranium phosphate. *Chem. Commun.* **2001**, *22*, 2378–2379. [CrossRef] [PubMed]
20. Locock, A.J.; Burns, P.C. Structures and syntheses of layered and framework amine-bearing uranyl phosphate and uranyl arsenates. *J. Solid State Chem.* **2004**, *177*, 2675–2684. [CrossRef]
21. Yu, Y.; Zhan, W.; Albrecht-Schmitt, T.E. One- and two-dimensional silver and zinc uranyl phosphates containing bipyridyl ligands. *Inorg. Chem.* **2007**, *46*, 10214–10220. [CrossRef]
22. Jouffret, L.; Rivenet, M.; Abraham, F. A new series of pillared uranyl-vanadates based on uranophane-type sheets in the uranium-vanadium-linear alkyl diamine system. *J. Solid State Chem.* **2010**, *183*, 84–92. [CrossRef]
23. Jouffret, L.; Shao, Z.; Rivenet, M.; Abraham, F. New three-dimensional inorganic frameworks based on the uranophane-type sheet in monoamine templated uranyl-vanadates. *J. Solid State Chem.* **2010**, *183*, 2290–2297. [CrossRef]
24. Alekseev, E.V.; Krivovichev, S.V.; Depmeier, W. A crown ether as template for microporous and nanostructured uranium compounds. *Angew. Chem. Int. Ed.* **2008**, *47*, 549–551. [CrossRef] [PubMed]
25. Bharara, M.S.; Gorden, A.E.V. Amine templated two- and three-dimensional uranyl sulfates. *Dalton Trans.* **2010**, *39*, 3557–3559. [CrossRef] [PubMed]
26. Doran, M.; Norquist, A.J.; O'Hare, D. $[NC_4H_{12}]_2[(UO_2)_6(H_2O)_2(SO_4)_7]$: The first organically templated actinide sulfate with a three-dimensional framework structure. *Chem. Commun.* **2002**, 2946–2947. [CrossRef] [PubMed]
27. Ling, J.; Sigmon, G.E.; Ward, M.; Roback, N.; Burns, P.C. Syntheses, structures, and IR spectroscopic characterization of new uranyl sulfate/selenate 1D-chain, 2D-sheet and 3D-framework. *Z. Kristallogr.* **2010**, *225*, 230–239. [CrossRef]
28. Siidra, O.I.; Nazarchuk, E.V.; Bocharov, S.N.; Depmeier, W.; Kayukov, R.A. Microporous uranyl chromates successively formed by evaporation from acidic solution. *Z. Kristallogr. Cryst. Mater.* **2018**, *233*, 1–8. [CrossRef]
29. Belova, L.N. *The Oxidation Zone of Hydrothermal Uranium Deposits*; Nedra Publishers: Moscow, Russia, 1975.
30. Hazen, R.M.; Ewing, R.C.; Sverjensky, D.A. Evolution of uranium and thorium minerals. *Am. Mineral.* **2009**, *94*, 1293–1311. [CrossRef]
31. Nash, K.L.; Madic, C.; Mathur, J.N.; Lacquemont, J. Actinide Separation Science and Technology. In *Chemistry of the Actinide and Transactinide Elements*; Morss, L.R., Edelstein, N.M., Fuger, J., Eds.; Springer: Dordrecht, The Netherlands, 2006; Volume 3, pp. 2644–2666.
32. Runde, W.; Neu, M.P. *The Chemistry of the Actinide and Transactinide Elements*; Morss, L.R., Edelstein, N.M., Fuger, J., Eds.; Springer: Dordrecht, The Netherlands, 2010; Volume 1. [CrossRef]
33. Burns, P.C.; Ewing, R.C.; Hawthorne, F.C. The crystal chemistry of hexavalent uranium: Polyhedron geometries, bond-valence parameters, and polymerization of polyhedra. *Can. Miner.* **1997**, *35*, 1551–1570.
34. Brown, I.D.; Altermatt, D. Bond-valence parameters obtained from a systematic analysis of the inorganic crystal structure database. *Acta Cryst.* **1985**, *41*, 244–247. [CrossRef]
35. Siidra, O.I.; Nazarchuk, E.V.; Charkin, D.O.; Bocharov, S.N.; Sharikov, M.I. Uranyl sulfate nanotubules templated by *N*-phenylglycine. *Nanomaterials* **2018**, *8*, 216. [CrossRef]
36. Tabachenko, V.V.; Kovba, L.M.; Serezhkin, V.N. Crystal structures $Mg(UO_2)_6(MoO_4)_7(H_2O)_{18}$ and $Sr(UO_2)_6(MoO4)_7(H_2O)_{15}$. *Khoord Khim.* **1984**, *10*, 558–562.
37. Gurzhiy, V.V.; Tyumentseva, O.S.; Krivovichev, S.V.; Tananaev, I.G. Selective Se-for-S substitution in Cs-bearing uranyl compounds. *J. Solid State Chem.* **2017**, *248*, 126–140. [CrossRef]
38. Krivovichev, S.V.; Cahill, C.L.; Burns, P.C. Syntheses and crystal structures of two topologically related modifications of $Cs_2[(UO_2)_2(MoO_4)_3]$. *Inorg. Chem.* **2002**, *41*, 34–39. [CrossRef] [PubMed]
39. Siidra, O.I.; Nazarchuk, E.V.; Kayukov, R.A.; Bubnova, R.S.; Krivovichev, S.V. $Cr^{VI} \rightarrow Cr^{V}$ transition in uranyl chromium compounds: Synthesis and high-temperature X-ray diffraction study of $Cs_2[(UO_2)_2(CrO_4)_3]$. *Z. Anorg. Allg. Chem.* **2013**, *639*, 2302–2306. [CrossRef]
40. Jouffret, L.J.; Wylie, E.M.; Burns, P.C. Amine templating effect absent in uranyl sulfates synthesized with 1,4-*n*-butyldiamine. *J. Solid State Chem.* **2013**, *197*, 160–165. [CrossRef]
41. Betke, U.; Wickleder, M. Oleum and sulfuric acid as reaction media: The actinide examples $UO_2(S_2O_7)$-lt (low temperature), $UO_2(S_2O_7)$-ht (high temperature), $UO_2(HSO_4)_2$, $An(SO_4)_2$ (An = Th, U), $Th_4(HSO_4)_2(SO_4)_7$ and $Th(HSO_4)_2(SO_4)$. *Eur. J. Inorg. Chem.* **2012**, *2012*, 306–317. [CrossRef]